# §48. Target Design with Fast Electron Beam Guiding by Strong Magnetic Fields

Sakagami, H.,
Johzaki, T. (Hiroshima Univ.),
Sunahara, A. (Institute for Laser Technology),
Nagatomo, H. (Inst. of Laser Engineering, Osaka Univ.),
Taguchi, T. (Setsunan Univ.),
Mima, K. (GPI)

A fuel target is imploded by long-pulse implosion lasers and its compressed core is heated by a short-pulse ultrahigh-intense laser in the fast ignition scheme. Incorporated fast ignition experiments have started at ILE, Osaka University to demonstrate that the compressed core could be heated up to 5 keV using Au cone-guided targets under the FIREX project. First series of the incorporated experiments was performed in 2009, and only 30-fold enhancement in neutron yield was achieved, and lower energy coupling from the heating laser to the imploded core was suspected.

2D PIC simulations indicate that even the coupling efficiency from the heating laser to fast electrons is generally high (> 40 %) but the divergence angle of fast electrons is large (~ 90 degree), and it results in low coupling efficiency from fast electrons to the core.[1)] To mitigate this critical issue, advanced target designs, in which external-compressed[2)] and/or self-generated[1,3,4)] strong magnetic fields are expected to guide fast electrons to the core, are proposed.

To investigate effects of the strong external longitudinal magnetic field on fast electron characteristics, the carbon (A = 12, Z = 6) target is introduced as a 20 μm thickness, 20 (±10) μm wide, $100n_{cr}$ flat profile with a preformed plasma, which has a exponential profile of the scale length ($L_{pre}$ = 1 μm) with density from 0.1 to $100n_{cr}$ in 2D PIC simulations. The heating laser is set to $\lambda_L$ = 1.06 μm, $\phi_{FWHM}$ = 5 μm, $\tau_{rise/fall}$ = 33 fs, $\tau_{flat}$ = 100 fs, and $I_L$ = $10^{19}$ W/cm$^2$. In experiments, the external magnetic field is initially induced by a capacitor-coil target[5)] and it is amplified by compression during the implosion. To mimic this external magnetic field, longitudinal (x-direction) magnetic fields ($B_{x,ext}$) are uniformly introduced into the plasma as the initial condition. The generated fast electrons are observed at the target surface.

The transverse momentum distributions ($p_y$, $p_z$) of fast electrons are shown in Fig. 1 for $B_{x,ext}$ = 0, 1 or 10 kT. The momentum spread along the laser magnetic field direction (z-direction) is negligible in the case without the external magnetic field ($B_{x,ext}$ = 0). When the external magnetic field is introduced, electrons gyrate in the plane perpendicular to the external magnetic field. Thus, the spread in y-direction (laser polarization direction) becomes smaller, and that in z-direction larger. The momentum distributions in $p_x$-$p_t$ plane, where $p_t = (p_y^2+p_z^2)^{1/2}$, are shown in Fig. 2 for $B_{x,ext}$ = 0, 1 or 10 kT. Comparing with the case without the external magnetic field, the angular spread in the transverse direction becomes larger for the case with the external fields. The number of fast electrons having the momentum along x-axis is reduced because of additional gyration motion. Even these results indicate that the external magnetic field enhances the angular spread in the momentum space, we can expect the suppression of spatial divergence of fast electrons. The spatial profiles of fast electron energy density observed at t = 176 fs are shown in Fig. 3 for $B_{x,ext}$ = 0, 1 or 10 kT. In the case without the external magnetic field, the fast electron beam spatially diverges. On the other hand, fast electrons are guided by the external magnetic fields and flow along the magnetic field lines. For the case with the sufficiently strong external magnetic fields, the Larmor radius becomes smaller with increasing $B_{x,ext}$, which results in smaller spatial divergence.

This work was partially supported by JSPS Grant-in-Aid for Scientific Research (C)(22540511) and (25400534).

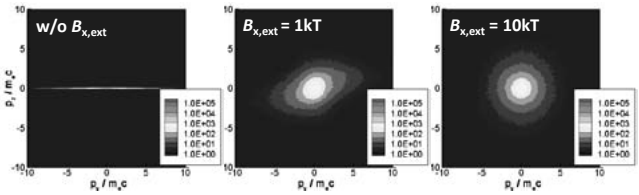


Fig. 1. Fast electron momentum distributions in transverse plane ($p_y$,$p_z$) for $B_{x,ext}$ = 0, 1, 10 kT.

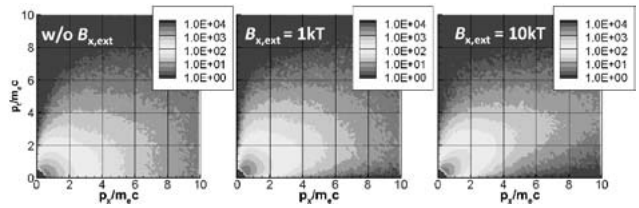


Fig. 2. Fast electron momentum distributions in $p_x$-$p_t$ plane, where $p_t = (p_y^2+p_z^2)^{1/2}$ for $B_{x,ext}$ = 0, 1, 10 kT.

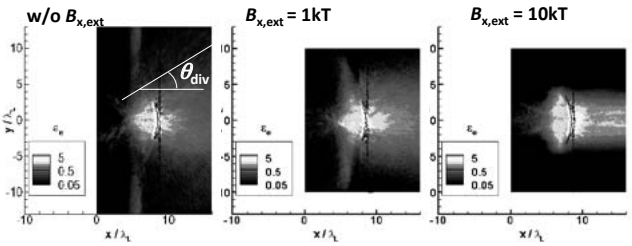


Fig. 3. Spatial profiles of fast electron energy density at t = 176 fs for $B_{x,ext}$ = 0, 1, 10 kT.

1) Johzaki, T., et al., Nucl. Fusion **51** (2011) 073022.
2) Strozzi, D. J. et al., Phys. Plasmas **19** (2012) 072711.
3) Norreys, P. A., et al., Plasma Phys. Control. Fusion **52** (2010) 124046.
4) Johzaki, T., et al., EPJ Web of Conferences **59** (2013) 03010.
5) Fujioka, S., et al., Sci. Report **3** (2013) 1170.